Experimental demonstration of non-iterative interpolation-based partial ICI compensation in100G RGI-DP-CO-OFDM transport systems

Mohammad E. Mousa-Pasandi,* Qunbi Zhuge, Xian Xu, Mohamed M. Osman, Ziad A. El-Sahn, Mathieu Chagnon, and David V. Plant

Photonic Systems Group, Department of Electrical and Computer Engineering, McGill University, Montreal, QC, H3A-2A7, Canada

me.mousapasandi@mail.mcgill.ca

Abstract: We experimentally investigate the performance of a low-complexity non-iterative phase noise induced inter-carrier interference (ICI) compensation algorithm in reduced-guard-interval dual-polarization coherent-optical orthogonal-frequency-division-multiplexing (RGI-DP-CO-OFDM) transport systems. This interpolation-based ICI compensator estimates the time-domain phase noise samples by a linear interpolation between the CPE estimates of the consecutive OFDM symbols. We experimentally study the performance of this scheme for a 28 Gbaud QPSK RGI-DP-CO-OFDM employing a low cost distributed feedback (DFB) laser. Experimental results using a DFB laser with the linewidth of 2.6 MHz demonstrate 24% and 13% improvement in transmission reach with respect to the conventional equalizer (CE) in presence of weak and strong dispersion-enhanced-phase-noise (DEPN), respectively. A brief analysis of the computational complexity of this scheme in terms of the number of required complex multiplications is provided. This practical approach does not suffer from error propagation while enjoying low computational complexity.

OCIS codes: (060.4080) Modulation; (060.1660) Coherent communications.

References and links

1. W. Shieh, H. Bao, and Y. Tang, "Coherent optical OFDM: theory and design," Opt. Express **16**(2), 841–859 (2008).
2. X. Liu and F. Buchali, "Intra-symbol frequency-domain averaging based channel estimation for coherent optical OFDM," Opt. Express **16**(26), 21944–21957 (2008).
3. F. Buchali, R. Dischler, and X. Liu, "Optical OFDM: a promising high-speed optical transport technology," Bell Syst. Tech. J. **14**, 127–148 (2009).
4. S. L. Jansen, B. Spinnler, I. Morita, S. Randel, and H. Tanaka, "100GbE: QPSK versus OFDM," J. Opt. Fiber Technol. **15**(5-6), 407–413 (2009).
5. S. L. Jansen, I. Morita, T. Schenk, N. Takeda, and H. Tankada, "Coherent optical 25.8-Gb/s OFDM transmission over 4160-km SSMF," J. Lightwave Technol. **26**(1), 6–15 (2008).
6. M. E. Mousa-Pasandi and D. V. Plant, "Zero-overhead phase noise compensation via decision-directed phase equalizer for coherent optical OFDM," Opt. Express **18**(20), 20651–20660 (2010).
7. C. Yang, F. Yang, and Z. Wang, "Orthogonal basis expansion-based phase noise estimation and suppression for CO-OFDM systems," IEEE Photon. Technol. Lett. **22**(1), 51–53 (2010).
8. Q. Zou, A. Tarighat, and A. H. Sayed, "Compensation of phase noise in OFDM wireless systems," IEEE Trans. Signal Process. **55**(11), 5407–5424 (2007).
9. L. Tomba, "On the effect of Wiener phase noise in OFDM systems," IEEE Trans. Commun. **46**(5), 580–583 (1998).
10. Y. Mostofi and D. C. Cox, "ICI mitigation for pilot-aided OFDM mobile systems," IEEE Trans. Wirel. Comm. **4**(2), 765–774 (2005).
11. Q. Zhuge, C. Chen, and D. V. Plant, "Dispersion-enhanced phase noise effects on reduced-guard-interval CO-OFDM transmission," Opt. Express **19**(5), 4472–4484 (2011).
12. M. E. Mousa-Pasandi and D. V. Plant, "Non-iterative interpolation-based partial phase noise ICI mitigation for CO-OFDM transport systems," IEEE Photon. Technol. Lett. **23**(21), 1594–1596 (2011).

#167812 - $15.00 USD Received 1 May 2012; revised 28 May 2012; accepted 29 May 2012; published 18 Jun 2012

13. M. E. Mousa Pasandi and D. V. Plant, "Non-iterative interpolation-based phase noise ICI mitigation for CO-OFDM transport systems," in Signal Processing in Photonic Communications, OSA Technical Digest (CD) (Optical Society of America, 2011), paper SPMB6.
14. P. Rabiei, W. Namgoong, and N. Al-Dhahir, "A non-iterative technique for phase noise ICI mitigation in packet-based OFDM systems," IEEE Trans. Signal Process. **58**(11), 5945–5950 (2010).
15. K. Kikuchi and K. Igarashi, "Characterization of semiconductor-laser phase noise with digital coherent receivers," in Optical Fiber Communication Conference, OSA Technical Digest (CD) (Optical Society of America, 2011), paper OML3.
16. X. Chen, A. Al Amin, and W. Shieh, "Characterization and monitoring of laser linewidths in coherent systems," J. Lightwave Technol. **29**(17), 2533–2537 (2011).
17. Q. Zhuge, M. E. Mousa-Pasandi, M. Morsy-Osman, X. Xu, M. Chagnon, Z. A. El-Sahn, and D. V. Plant, "Demonstration of dispersion-enhanced phase noise in RGI CO-OFDM systems," IEEE Photon. Technol. Lett. ((submitted to).
18. B. Spinnler, "Equalizer Design and Complexity for Digital Coherent Receivers," IEEE J. Sel. Top. Quantum Electron. **16**(5), 1180–1192 (2010).

1. Introduction

Coherent optical orthogonal frequency division multiplexing (CO-OFDM) transmission systems have been intensively investigated as a promising candidate for Ethernet transport at 100 Gb/s and beyond [1–3]. Although OFDM was originally designed for wireless transmission, recently, it has received a great deal of attention in optical communications. This is because of its ease of equalization and therefore, robustness with respect to the fiber transmission impairments such as chromatic dispersion (CD) and polarization mode dispersion (PMD) [1,4]. OFDM transmits high-speed serial information through multiple lower-speed sub-channels. This reduction in the baud-rate leads to a reduction in inter-symbol interference (ISI) and therefore a simplification of the equalization process at the receiver. However, the performance of coherent transmission systems are known to suffer from laser phase noise and in the case of CO-OFDM systems, the degradation is more pronounced considering the relatively longer symbol duration with respect to single carrier (SC) schemes. This ultimately would limit the transmission reach and consequently make the use of low linewidth laser sources inevitable.

In CO-OFDM, laser phase noise degrades the received signal quality in two ways— the common phase error (CPE), which is an identical phase rotation for all subcarriers, and the inter-carrier interference (ICI), which is due to the loss of orthogonality between subcarriers. In optical communication transmission systems, laser phase noise compensation schemes may use RF-pilot enabled [5], pilot subcarrier (PSC) enabled [1–3], decision-directed and maximum likelihood (ML) algorithms [1,6] in which except for the RF-pilot enabled algorithm, all could only mitigate the CPE. However, for relatively large laser linewidths and/or longer symbol durations the degradation due to ICI becomes pronounced and needs to be compensated. In [7], the authors adopted an orthogonal basis expansion-based technique to suppress both CPE and ICI in CO-OFDM systems. In wireless, the effect of ICI on the performance of OFDM systems due to the local oscillator (LO) phase noise has been extensively investigated and several iterative algorithms have been proposed to jointly estimate the data and the phase noise vector [8–10]. Nevertheless, since ICI mitigation requires de-convolving the phase noise spectral components from unknown data subcarriers, such iterative schemes suffer from large latency and high implementation complexity making them unsuitable for long-haul ultra high-speed optical transmission applications.

On the other hand, unlike conventional CO-OFDM systems, reduced-guard-interval CO-OFDM (RGI-CO-OFDM) systems experience dispersion-enhanced-phase-noise (DEPN) due to the LO as the CD induced walk-off becomes comparable to the OFDM symbol length. Therefore, as shown in [11], the same induced phase noise process would degrade the signal quality more if applied at the receiver as the LO. The grouped-maximum-likelihood (GML) phase estimation approach is known to partially mitigate the DEPN impairment [11].

Recently in [12,13], we numerically investigated the feasibility of a partial ICI compensation scheme based on a linear interpolation between the CPE estimates of consecutive OFDM symbols for CO-OFDM transport systems. It is shown in [14] that this approach can minimize the mean square error (MSE) of the estimated interpolation of the time-domain phase noise

#167812 - $15.00 USD Received 1 May 2012; revised 28 May 2012; accepted 29 May 2012; published 18 Jun 2012

samples. In this paper, we experimentally investigate the performance of the interpolation-based ICI compensator in a 112 Gb/s reduced-guard-interval dual-polarization coherent-optical orthogonal-frequency-division-multiplexing (RGI-DP-CO-OFDM) transmission systems, employing a low-cost distributed feedback (DFB) laser. To study the performance of the interpolation-based ICI compensator, two different scenarios are considered: a) a DFB laser with the linewidth of 2.6 MHz at the transmitter and an external-cavity-laser (ECL) with the linewidth of less than 100 kHz at the receiver, emulating weak DEPN; and b) the ECL at the transmitter and the DFB laser at the receiver, emulating strong DEPN. Considering a bit error rate (BER) value of 1×10^{-3} as the forward error correction (FEC) threshold, for the case with weak DEPN, a transmission distance of 2300 km over single mode fiber (SMF) was achieved demonstrating a 24% increase in transmission reach with respect to a system employing a conventional equalizer (CE). In the presence of strong DEPN, a reach of 2300 km was achieved when our ICI compensator was combined with a grouped-maximum-likelihood algorithm [14], representing a 13% improvement compared to a system without ICI compensation. Moreover, we provide a brief comparison of the computational complexity of the proposed ICI compensation scheme and the CE in terms of the number of complex multiplications. The computational complexity for the case of the parameters of our experiment in this paper is only 25% in terms of the number of complex multiplications compared to the CE.

This paper is structured as follows. We briefly explain the principle of the interpolation-based ICI compensation in section 2. In section 3, we review our RGI-DP-CO-OFDM experimental setup and study the performance of interpolation-based ICI compensator. In section 4, the complexity of this algorithm is studied and section 5 concludes the paper.

2. The concept of interpolation-based ICI compensation

The effect of phase noise on OFDM samples in time-domain is modeled as a multiplication which can be equivalently expressed as a convolution in the frequency-domain

$$r_k^m = \sum_{q=0}^{N-1} p_{\langle k-q \rangle}^m h_q x_q^m + w_k^m = p_0^m h_k x_k^m + \sum_{q=0, q \neq k}^{N-1} p_{\langle k-q \rangle}^m h_q x_q^m + w_k^m \qquad (1)$$

where x, p, h and r are the subcarrier-specific transmitted data symbol in frequency-domain, the phase noise spectral components, the subcarrier-specific channel frequency response and the subcarrier-specific received data symbol in frequency-domain, respectively. k and m denote the subcarrier (frequency) and symbol (time) indexes, respectively and w represents the additive noise. As seen in Eq. (1), P_0^m is the common term, affecting every subcarrier and therefore, based on the definition, it reflects the CPE contribution. The existence of other phase noise harmonics in Eq. (1) causes the ICI and estimating these harmonics is the key to ICI compensation. The interpolation-based ICI compensator performs the next three steps:

Step1. Similar to the CE, scattered pilot subcarriers are used to estimate the CPE in every OFDM data symbol as

$$CPE^m = p_0^m = angle\left\{ r_k^m \times conj\left(h_k x_k^m \right) \right\} \qquad k \in PSC \qquad (2)$$

This estimated CPE value is set equal to the phase noise corresponding to the middle time-domain sample of the same data symbol.

Step 2. The phase noise values of the remaining intermediate samples of each symbol in the time-domain are determined by a linear interpolation using the CPE estimates of the previous, current and next OFDM symbols. This linear interpolation provides the optimum MSE interpolation as long as $\beta T_s << 1$, where β and T_s are the two-sided 3-dB bandwidth of the phase noise process and the symbol duration, respectively [14]. Consequently, the equalization of the m^{th} received symbol can be completed only after reception of the $(m + 1)^{th}$ symbol. Therefore, the interpolation-based ICI compensator requires a one-symbol buffer, resulting in a one-symbol latency.

#167812 - $15.00 USD Received 1 May 2012; revised 28 May 2012; accepted 29 May 2012; published 18 Jun 2012

Step 3. After the time-domain phase noise vector is approximated by a linear interpolation between consecutive OFDM symbols in step 2, we can derive the spectral components of phase noise estimation by the Fourier transform operation. Then, the received symbol can be equalized as

$$\hat{x}_k^m = \left(\sum_{l=-Q/2}^{Q/2} conj\left(\hat{p}_{\langle l \rangle}^i \right) \times r_{\langle k-l \rangle}^m \right) \Big/ \hat{h}_k \tag{3}$$

where the notion of ^ indicates that the corresponding parameter is based on an estimation. $\hat{p}$ represents the spectral components of estimated phase noise in which the total number of spectral components that are taken into account is controlled by the parameter Q. As Eq. (3) indicates, instead of de-rotating the OFDM samples in time-domain, the receiver can simply convolve the received symbol by the spectral components of the estimated phase noise followed by a one-tap frequency-domain equalizer. Since laser phase noise can be approximately expressed as a Wiener process and most of the energy of a Wiener process is concentrated in the first few harmonics, a small value for Q can be adopted to reduce the required number of complex multiplications in Eq. (3).

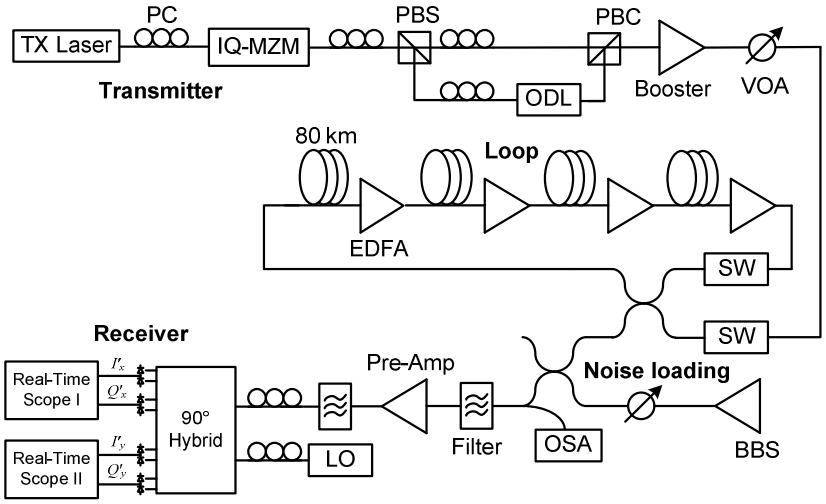

Fig. 1. RGI-DP-CO-OFDM experimental setup.

3. Performance of interpolation-based ICI compensator in RGI-DP-CO-OFDM systems

Figure 1 depicts the experimental setup. The original binary pseudo-random bit sequence (PRBS) data with the length of 2^{17}-1 is first divided and mapped onto 224 frequency subcarriers with QPSK modulation format and subsequently transferred to the time-domain by an IFFT of size 256 while zeros occupy the remainder, fixing the value 1.14 as the oversampling ratio. In this RGI-DP-CO-OFDM system, a cyclic prefix of length 8, 2 pilot symbols for every 50 data symbols and 4 pilot subcarriers are employed. The in-phase (I) and quadrature (Q) parts of the resulting digital OFDM signal are then loaded separately on two field-programmable gate arrays (FPGAs) to electrically generate the electrical I and Q via two digital to analogue convertors (DACs), operating at 32 GS/s. Considering the oversampling ratio of 1.14, the analogue electrical I and Q signals at 28 Gbaud OFDM are generated and then fed into an IQ Mach-Zehnder modulator (IQ-MZM). Right after the IQ-MZM, a dual polarization emulator is used to imitate a dual-polarization multiplexed transmitter. The optical transmission link consists of a 4-span optical recirculating loop with uncompensated SMF with the dispersion parameter of 17 ps/nm.km, the nonlinear coefficient of 1.2 $W^{-1}.km^{-1}$ and the loss parameter of 0.18 dB/km. Spans are 80 km long and separated by erbium-doped-fiber-

#167812 - $15.00 USD Received 1 May 2012; revised 28 May 2012; accepted 29 May 2012; published 18 Jun 2012

amplifiers (EDFAs) with a noise figure of ~6 dB. At the optical receiver, two optical filters with the bandwidths of 0.4 nm and 0.8 nm are applied before and after the preamplifier, respectively, to reject the out-of-band accumulated spontaneous emission (ASE) noise. The receiver is based on the intradyne scenario in which the received signal beats with the optical LO signal in an optical polarization-diversity 90° hybrid to obtain the signal I and Q components. The LO is tuned to within the range of approximately tens of MHz of the received signal's center frequency. The four pairs of balanced outputs from the hybrid are then detected by four balanced photodetectors and then electrically sampled and asynchronously digitized at 80 GSamples/s using two commercial 4-channel real-time oscilloscopes, equipped with analog-to-digital converters (ADCs) characterized by 33 GHz of analogue bandwidth, a nominal resolution of 8-bit and a frequency-dependent effective number of bits (ENoB) between 4 and 5. Four signals are then transferred to PC for off-line processing. In off-line processing, an inter subcarrier frequency averaging (ISFA) algorithm with an averaging parameter of 9 and a ML phase estimation were incorporated [1,2].

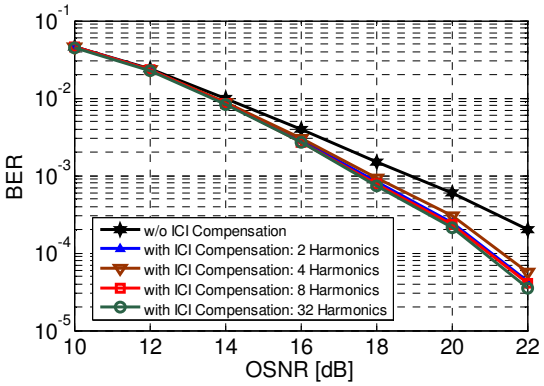

Fig. 2. BER versus OSNR for different ICI estimation harmonics. The DFB laser is employed at the transmitter.

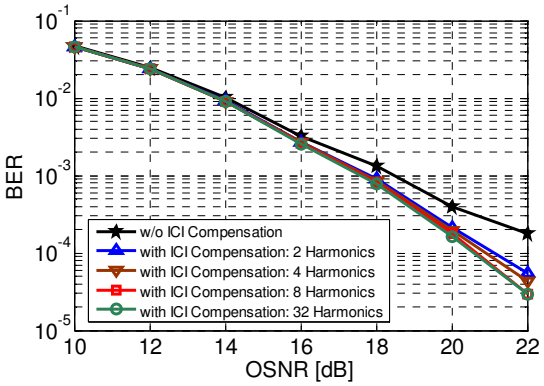

Fig. 3. BER versus OSNR for different ICI estimation harmonics. The DFB laser is employed at the receiver.

The linewidth of the ECL was less than 100 kHz. For the DFB laser used in the experiment, we measured the laser phase noise variance σ_φ^2 using a coherent detection algorithm as described in [15,16] with an averaging window of 50 symbols and a relative delay of 50 symbols. The measured data was then converted to linewidth Δf using $\Delta f = \sigma_\varphi^2 / 2\pi T$ where T represents the symbol duration, assuming the laser phase noise as a Wiener process [15,16].

#167812 - $15.00 USD Received 1 May 2012; revised 28 May 2012; accepted 29 May 2012; published 18 Jun 2012

Figure 2 and Fig. 3 study the BER performance of the interpolation-based ICI compensator versus optical-signal-to-noise-ratio (OSNR) at optical back-to-back (B2B) for a different number of estimated phase noise spectral components (harmonics). In Fig. 2, the DFB laser is employed at the transmitter and in Fig. 3, the DFB laser is used at the receiver. The performance of the ICI compensator would improve by increasing the number of estimated phase noise spectral components. Nevertheless, considering that most of the energy of the phase noise process is concentrated in the first few harmonics, the major signal quality improvement is observed for the first few harmonics. As one can see, the higher the OSNR, the more effective the ICI compensator performs. The ICI compensator always provides a better signal quality than CE (or similar for lower OSNR) across the received OSNR range of study. This confirms that it does not suffer from error propagation even in noisy scenarios. We choose a harmonic number of 8 for further studies in the rest of this paper. Furthermore, Fig. 2 and Fig. 3 show very similar performances as DEPN does not exist in case of B2B (no dispersion).

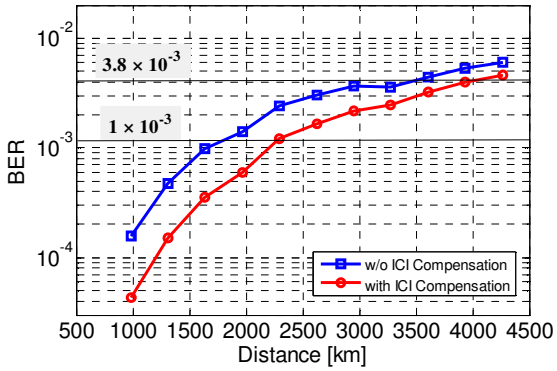

Fig. 4. BER versus distance where the DFB laser is employed at the transmitter (weak DEPN).

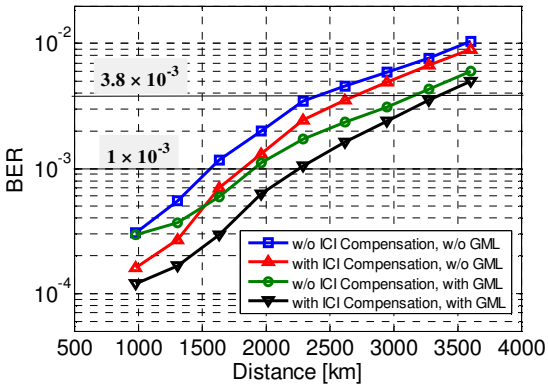

.0

Fig. 5. BER versus distance where the DFB laser is employed at the receiver (strong DEPN).

Figure 4 compares the BER performance of the interpolation-based ICI compensator and the CE versus transmission distance in the presence of weak DEPN. The DFB laser and the ECL were used at the transmitter and the receiver, respectively. Blue and red curves correspond to the equalization without and with ICI compensation, respectively. As one can see, the ICI compensator, red curve, shows a better performance than the CE, blue curve, achieving a transmission reach of 2300 km at the BER threshold of 1×10^{-3}, demonstrating a transmission reach improvement of 24%. In Fig. 5, we again study the BER performance of the ICI compensator and the CE versus transmission distance however, this time, the ECL is used at transmitter and the DFB laser is employed at receiver, stimulating the strong DEPN effect.

#167812 - $15.00 USD Received 1 May 2012; revised 28 May 2012; accepted 29 May 2012; published 18 Jun 2012

Blue and red curves correspond to the equalization without and with ICI compensation, respectively. Comparing Fig. 4 and Fig. 5, a significant degradation in the transmission reach is observed due to the strong DEPN effect. However, the ICI compensator, red curve, still provides a better performance than the CE, blue curve, achieving a transmission reach of 1800 km at the BER threshold of 1×10^{-3}, demonstrating a transmission reach improvement of 13%.

In [11,17], the GML algorithm was proposed to compensate for the DEPN impairment. We applied the ICI compensation scheme in conjunction with the GML algorithm to further study its behavior. Green and black curves correspond to the GML equalization without and with ICI compensation, respectively. As can be seen in Fig. 5, the ICI compensator in conjunction with the GML algorithm, black curve, improves the transmission reach by 13%, providing 2300 km reach.

4. System complexity

The complexity of an equalization algorithm directly affects the implementation cost of the transmission link because of hardware costs and power consumption. In this section, we provide a brief comparison of the complexity of the interpolation-based ICI compensator and the CE in terms of the number of required complex multiplications per bit, taking into account the FFT operations, and the channel estimation and equalization. In this study, the same complexity for multiplication and division is considered. Assume that the channel is estimated every N_{CE} symbols and R_{CE} is the training symbol overhead. M denotes the number of bits per symbol. As is shown in [18], the complexity of the CE in an RGI-DP-CO-OFDM system, C_{CE}, can be expressed as

$$C_{CE} = \frac{N_1\left(\log_2\left(N_1\right)+1\right)n'_{MC}}{\left(N_1 - N_{CD}+1\right)\log_2\left(M\right)} + \frac{n_{MC}\log_2\left(N_2\right)+2+\dfrac{5}{N_{CE}R_{CE}}}{\log_2\left(M\right)} \tag{4}$$

where N_1, N_2, n_{MP} and n'_{MP} are the FFT lengths of the first static frequency-domain equalization (FDE), FFT lengths of the second adaptive FDE, OFDM oversampling ratio and modified FDE oversampling ratio, respectively N_{CD} represents the minimum number of equalizer taps necessary to compensate chromatic dispersion (CD) [18]. The interpolation-based ICI compensator has similar complexity regarding channel estimation however, one more FFT operation per symbol is required to derive the phase noise spectral components from the estimated time-domain phase noise samples. This can be realized by $N_3\log_2\left(N_3\right)/2$ complex multiplications per symbol for each polarization where N_3 is the corresponding FFT size. A Q-point FFT ($N_3 = Q$) provides the least complexity. Moreover the equalization is performed based on Eq. (3) resulting in $QN_2\left(1-R_{CE}\right)/n_{MC}$ more complex multiplications per symbol per polarization to de-convolve the estimated phase noise spectral harmonics. Assuming that for each polarization, every symbol transmits $N_2\log_2\left(M\right)/n_{MC}$ bits then, the total complexity for interpolation-based ICI compensator, C_{ICI}, reduces to

$$\begin{aligned} C_{ICI} &= \frac{N_1\left(\log_2\left(N_1\right)+1\right)n'_{MC}}{\left(N_1 - N_{CD}+1\right)\log_2\left(M\right)} + \frac{n_{MC}\log_2\left(N_2\right)+2+\dfrac{5}{N_{CE}R_{CE}}}{\log_2\left(M\right)} + \frac{QN_2\left(1-R_{CE}\right)/n_{MC}+N_3\log_2\left(N_3\right)}{N_2\log_2\left(M\right)} \\ &= C_{CE} + \frac{QN_2\left(1-R_{CE}\right)/n_{MC}+N_3\log_2\left(N_3\right)/2}{N_2\log_2\left(M\right)} \end{aligned} \tag{5}$$

#167812 - $15.00 USD Received 1 May 2012; revised 28 May 2012; accepted 29 May 2012; published 18 Jun 2012

For retrieving the spectral components of the estimated phase noise, although a relatively small FFT size, N_3, offers less complexity, the aliasing effect can reduce the improvement. We investigated and empirically observed that an FFT size of 4Q points guarantees negligible aliasing effect which does not compromise the ICI mitigation.

Considering the fact that a small value can be adopted as the parameter Q, as we have seen in Fig. 2 and Fig. 3, the overall complexity of the interpolation-based ICI compensator can be quite low. For the case of this experiment and considering 8 harmonics and a 4Q-point FFT for ICI compensation, we observe a complexity of 25% in terms of the number of complex multiplications.

5. Conclusion

In this paper, we investigated the performance of a non-iterative phase noise induced ICI compensator based on linear interpolation for OFDM transport systems. Experimental results demonstrated the signal quality improvement using this scheme for 112 Gb/s QPSK RGI-DP-CO-OFDM transmission over uncompensated link employing a low-cost DFB laser. An improvement of 24% and 13% in the transmission distance was observed in case of weak and strong presence of DEPN, respectively. Robustness to error propagation and low computational complexity are the main advantages of this approach. Using more sophisticated methods such as iterative algorithms and/or joint data and phase noise estimation can result in a better performance however, their associated implementation complexity with respect to the proposed interpolation-based ICI compensation is significantly higher.

Acknowledgments

The authors gratefully acknowledge the financial support from the Canadian Foundation for Innovation (CFI) and NSERC/Bell Canada Industrial Research Chair. Authors would like to thank Benoît Châtelain, Zhaoyi Pan and Jonathan Buset for their fruitful help. The VEGA DACs were supplied by Micram.

#167812 - $15.00 USD Received 1 May 2012; revised 28 May 2012; accepted 29 May 2012; published 18 Jun 2012